Published in final edited form as:
Invest Ophthalmol Vis Sci. 2006 April ; 47(4): 1491–1499.

Detection of Differentially Expressed Glycogenes in Trabecular Meshwork of Eyes with Primary Open-Angle Glaucoma

Shiri Diskin[1,2,3], **Janardan Kumar**[1,2,3], **Zhiyi Cao**[1], **Joel S. Schuman**[4], **Tim Gilmartin**[5], **Steven R. Head**[5], and **Noorjahan Panjwani**[1,2]

1 *New England Eye Center, Department of Ophthalmology, Tufts University School of Medicine, Boston, Massachusetts*

2 *Department of Anatomy and Cell Biology, Tufts Sackler School of Biomedical Sciences, Boston, Massachusetts*

4 *UPMC Eye Center, Department of Ophthalmology, University of Pittsburgh School of Medicine, Pittsburgh, Pennsylvania*

5 *DNA Array Core Facility, The Scripps Research Institute, La Jolla, California*

Abstract

Purpose—To identify differentially expressed glycogenes in trabecular meshwork (TM) of eyes with primary open-angle glaucoma (POAG).

Methods—Total RNA was isolated from TM of cadaveric eyes derived from donors with diagnosed glaucomas of different etiologies and from normal control subjects. RNA was amplified and hybridized to the GLYCOv2 oligonucleotide microarray that contains probes for carbohydrate-binding proteins, glycosyltransferases, and other genes involved in the regulation of glycosylation. Statistical analysis was used to identify differentially expressed genes between normal and POAG samples.

Results—This study revealed that POAG TM and normal TM have distinct gene expression profiles. Of the 2001 genes on the array, 19 genes showed differential expression of greater than 1.4-fold in POAG. Mimecan and activinA, which have been shown to be upregulated in models of glaucoma, were both found to be elevated in POAG TM. Many genes were identified for the first time to be differentially regulated in POAG. Among the upregulated genes were: (1) cell adhesion molecules including platelet endothelial cell adhesion molecule-1 and P-selectin, both of which are targets of NFκB, which has been shown to be activated in glaucomatous TM; (2) lumican, a core protein of keratan sulfate proteoglycans; and (3) the receptor for IL6, a cytokine that has been shown to be upregulated in TM in response to elevated intraocular pressure. Among the downregulated genes were chondroitin-4-O-sulfo-transferase involved in the synthesis of chondroitin sulfate chains and the receptor for PDGFβ, a growth factor that has been shown to stimulate both TM cell proliferation and phagocytic activity. Results for several genes were confirmed by RTq-PCR.

Corresponding author: Noorjahan Panjwani, Department of Ophthalmology, Tufts University School of Medicine, 136 Harrison Avenue, Boston, MA 02111; noorjahan.panjwani@tufts.edu.

[3]Contributed equally to the work and therefore should be considered equivalent authors.

Disclosure: **S. Diskin**, None; **J. Kumar**, None; **Z. Cao**, None; **J.S. Schuman**, None; **T. Gilmartin**, None; **S.R. Head**, None; **N. Panjwani**, None

Supported by National Eye Institute Grants EY015168 (NP) and EY13178 (JSS) and Core Grant EYP30-13078 for Vision Research, the Massachusetts Lions Eye Research Fund, the Eye and Ear Foundation (Pittsburgh), and Research to Prevent Blindness, Inc. The gene microarray analysis was conducted by the Gene Microarray (E) Core of The Consortium for Functional Glycomics funded by National Institute of General Medical Sciences Grant GM62116.

Conclusions—Microarray technology was used to show, for the first time, that POAG TM has a distinct glycogene expression profile. Differentially expressed glycogenes identified in this study have not been previously investigated for their role in the pathogenesis of POAG and thus are novel factors for further study of the mechanism of the disease and for their possible use as diagnostic markers.

The tissues of the aqueous outflow pathway and specifically the trabecular meshwork (TM) have long been thought to play a pivotal role in facilitating the outflow of aqueous humor and in maintaining proper intraocular pressure (IOP). Although the molecular mechanism responsible for the resistance to outflow in primary open-angle glaucoma (POAG) has not been elucidated, it is generally accepted that the integrity of the TM and proper function of TM cells are prerequisites for the maintenance of the normal outflow system. The need to identify functional differences between normal and glaucomatous TM cells has been recognized for many years, and a large body of research is geared toward finding these differences. To date, global comparisons of gene expression patterns using high-throughput methods such as microarrays have only been used to compare normal TM tissue or cultured cells with models of POAG. These models are cultured normal cells treated with glucocorticoid (dexamethasone)[1–3] or TGFβ[4] and whole TM tissue in organ culture perfused with high pressure.[5,6]

The survival of TM cells and their proper adhesion to the extracellular matrix (ECM) are crucial for their proper function and ability to maintain outflow facility. In nonocular studies, carbohydrate-based recognition systems have been implicated in cell death mechanisms[7–10] and in cell–cell and cell–ECM interactions.[9–14] This body of data, combined with the finding that E-selectin (ELAM-1), a carbohydrate-recognizing protein, is a marker for glaucomatous TM,[15] lead us to hypothesize that carbohydrate-based recognition systems are involved in the pathogenesis of POAG. To test this hypothesis, we used a glycogene microarray to compare glycogene expression profiles of whole TM tissues from normal and glaucomatous eyes obtained from human donors. The array contains probe sets for 2001 murine and human gene transcripts coding for carbohydrate-binding proteins, glycosyltransferases, glycosidases, and carbohydrate sulfotransferases—genes that are not well represented in most commercially available microarrays. The study revealed that POAG TM and normal TM have distinct glycogene expression profiles. We also have identified specific glycogenes whose differential expression in the diseased tissue may have an effect on the disease process. Among these are genes that are involved in ECM remodeling such as lumican, iduronate-2-sulfatase (IDS), and chondroitin-4-O-sulfotransferase, and cell adhesion molecules such as platelet endothelial cell adhesion molecule (PECAM)-1 and E- and P-selectins.

Materials and Methods

Tissue Handling and RNA Extraction

Ten pairs of human eyes from donors between 66 and 87 years of age (normal, $n = 4$; POAG, $n = 3$; low-tension glaucoma, $n = 1$; suspected glaucoma, $n = 2$; Table 1) were obtained from the Central Florida Lions Eye and Tissue Bank (Tampa, FL) or from the National Disease Research Interchange (Philadelphia, PA). Assignment of samples to study groups—normal, POAG, and non-POAG glaucoma—was based on diagnosis and medical information supplied by the donors' treating ophthalmologists through a detailed questionnaire distributed by the eye banks. The study was approved by the Tufts University Internal Review Board and was conducted in accordance with the Declaration of Helsinki and HIPAA (Health Insurance Portability and Accountability Act of 1996) regulations. Eyes were enucleated within 6 hours after death and preserved for RNA extraction (RNALater; Ambion, Austin, TX) after a ~1-cm slit was made at the equator. The trabecular mesh-work was dissected within 24 hours after death in a manner previously described[16] with extra care to avoid contamination of TM samples with iris, corneal, scleral, and ciliary body tissues. Immediately after dissection, tissues

were stored at −80°C until use. Total RNA was isolated from tissue with a kit (RNeasy; Qiagen, Chatsworth, CA), as described.[5] Briefly, frozen tissue was crushed on dry ice with a clean pestle; suspended in guanidine thiocyanate buffer (Buffer RLT, RNeasy kit; Qiagen) and loaded onto a column (QIAshredder; Qiagen). Eluent from the column was subjected to RNA extraction (RNeasy; Qiagen), and RNA molecules selectively bound to a silica gel base were eluted with 30 μL of RNAase-free water. The quality and yield of each RNA preparation was determined (Bioanalyzer 2100 with RNA Pico Lab-Chips; Agilent, Waldbronn, Germany).

Microarray Hybridization and Data Analysis

For preparation of hybridization probes, 100 ng of each RNA sample was subjected to two rounds of T7 RNA polymerase amplification according to a modified Baugh/Harvard protocol (http://www.scripps.edu/researchservices/dna_array/pdf%20files/Affymetrix%20Small%20Sample%20Protocol.pdf). The resultant product of the second round of cDNA synthesis was used as the starting material for in vitro transcription incorporating biotin labeled ribonucleotides. Labeled cRNA was fragmented, hybridized to GLYCOv2 microarrays, and scanned according to standard microarray protocols (Gene-Chip; Affymetrix, Santa Clara, CA). The glycogene microarray GLYCOv2 is an oligonucleotide microarray (Affymetrix) and was provided for our use by the Consortium for Functional Glycomics at the Scripps Institute. The array contains probe sets for 2001 murine and human gene transcripts coding for carbohydrate-binding proteins, glycosyltransferases, glycosidases, and carbohydrate sulfotransferases—genes that are involved in the regulation of glycosylation. In this array, transcripts are detected by three identical probe sets for each glycogene, each probe set consisting of 11 probe pairs. Each probe pair is made up of one 25-bp perfect-match oligonucleotide that matches the sequence of the targeted transcript and one oligonucleotide designed with a mismatch at the center position. In addition to probes for glycogenes, the array contains probes for selected cytokines, growth factors, and their receptors. A complete list of probe sets and annotation for the GLYCOv2 oligonucleotide array is available at http://www.functionalglycomics.org/static/consortium/resources/resourcecoree.shtml/.

Expression signal values were generated with the RMA algorithm (http://www.stat.berkeley.edu/~bolstad/RMAExpress/RMAExpress.html/), which models the performance of the perfect-match probe sets with all chips used in the study. This model is then used to calculate quantile normalized, background subtracted, base 2 log-transformed expression values for all probe sets used in the analysis.

Hierarchical clustering was preformed based on all analyzed genes using centered correlation and average linkage with the software BRB ArrayTools 3.2.2 (http://linus.nci.nih.gov/BRB-ArrayTools.html/ developed by Dr. Richard Simon and Amy Peng at the Biometric Research Branch of the National Cancer Institute, National Institutes of Health, Bethesda, MD). Changes in gene expression between the POAG and normal groups were determined by using the following methodologies.

Transformed expression values for replicated probe sets were averaged to generate a single expression value for each probe set. A detection call filter to remove absent genes from further analysis was not used in this study, because the two-round amplification protocol used in this study has been shown to be capable of inhibiting the ability of the GCOS algorithm to make present detection calls.[17] To identify statistically significant changes in gene expression, BRB ArrayTools 3.2.2 software was used for class comparison. The class comparison test was conducted with a univariate α-level cutoff of 0.05 and multivariate permutation-based false-discovery rate calculation. The predicted proportion of false discoveries was preset at 10%. A false-discovery rate calculation was set at a confidence level of 80%, assuming a β-risk of 0.2. Differentially expressed genes were visualized using Cluster and Tree View software packages for heat map creation (Eisen Laboratory, University of California Berkeley, Berkeley, CA;

http://rana.lbl.gov/EisenSoftware.htm). For this, each individual gene was compared with median unlogged RMA signal intensities, using the POAG and normal arrays in the study. Differences from the median were represented in varying intensities of green (decreased change [*x*-fold] compared with the median) and red (increased change compared with the median).

Differentially expressed genes were subjected to further analysis to gain insight into their biological functions. For this, the Database for Annotation, Visualization and Integrated Discovery (DAVID) software developed by the Laboratory of Immunopathogenesis and Bioinformatics at SAIC-Frederick, Inc. (http://apps1.niaid.nih.gov/david/National Institute of Allergy and Infectious Diseases, National Institutes of Health) was used.

Real-Time Quantitative RT-PCR

Real-time quantitative reverse transcription–polymerase chain reaction (RT-qPCR) was performed (Mx4000 real-time PCR machine; Stratagene, La Jolla, CA). The same total RNA extractions were used for both microarray and PCR analysis. Briefly, cDNA was synthesized from 25 ng total RNA (High Capacity kit; Applied Biosystems, Inc. [ABI], Foster City, CA), according to the manufacturer's instructions. Another kit was used for PCR amplification (Assays-on-Demand Gene Expression Products; ABI). PCR (*Taq*Man; ABI) was performed in duplicate or triplicate with 1.25 ng cDNA, inventory gene-specific primers (ABI), and master mix (*Taq*Man Universal PCR Master Mix; ABI) containing ROX as a passive reference, according to the manufacturer's instructions. Reactions performed in the absence of template served as the negative control. The specific ABI catalog numbers for primer sets used in this study include: *β*-actin: HS99999903_m1, E-selectin: HS00174057_m1, P-selectin: HS00174583_m1, ICAM1: HS00164932_m1, PECAM1: HS00169777_m1, activin A: HS00170103_m1, and lumican: HS00158940_m1. For amplification, after an initial denaturation step (95°C for 10 minutes) to activate the DNA polymerase (Amplitaq Gold; ABI), the reactions were subjected to 50 cycles involving denaturation (95°C for 15 seconds) and annealing plus extension (60°C for 1 minute). Fluorescent signals were recorded once per cycle with a detector corresponding to FAM. Data analysis was performed (Mx4000 software version 2; Stratagene). To normalize the non–PCR-related fluctuations between wells, we measured each fluorescent reporter signal against the ROX (internal reference dye) signal. An amplification plot showing the increase in the FAM fluorescence with each cycle of PCR (ΔRn) was generated for every sample. A threshold cycle value (C_t) was calculated from each amplification plot. The C_t represented the PCR cycle number at which fluorescence was detectable above an arbitrary threshold, based on the variability of the baseline data during the first 15 cycles. All C_ts were obtained in the exponential phase. Quantification data of each gene were normalized to the expression of *β*-actin which served as a positive amplification control. A value of 1.0 was assigned to the expression of each gene in the NTM 105 specimen which served as a calibrator. The expression values for all other specimens were calculated as change in expression level with respect to NTM 105.

Results

RNA Yield and Quality

Total RNA extracted from whole TM tissue was run on a bioanalyzer (model 2100; Agilent) for quantity and quality assessment. RNA extractions from whole TM tissues yielded between 90 and 1900 ng RNA/eye, with an overall tendency for lower yields in the POAG eyes (145 ± 56 ng/eye, $n = 3$), compared with other groups (normal: 280 ± 138 ng/eye, $n = 4$; non-POAG glaucoma: 1325 ± 513 ng/eye, $n = 3$). The yield of RNA was significantly higher from non-POAG eyes than from normal and POAG eyes, despite the extreme care taken to avoid contamination with ciliary, corneal, or scleral tissues. The quality of RNA was uniform across samples, with rRNA ratio (28S/18S) ranging between 1 and 1.2. In Figure 1 are representative

electropherograms and gel-like images showing that, in all samples, 18S and 28S gel bands and graph peaks are dominant and the amount of low-molecular-weight RNA is insignificant, indicating minimal RNA degradation in the samples. Although the 28S/18S ratio that is considered to represent the best RNA quality is 2:1, it has been reported that ratios as low as 0.4 are adequate for microarray hybridization, as long as RNA degradation is minimal and 28S and 18S RNA are the two major components detected in electropherograms.[18] Thus, all RNA preparations used in this study were deemed satisfactory for hybridization to the chips.

Hierarchical Clustering

To gain better understanding of the relationship between sample data sets, we used an unsupervised hierarchical clustering by sample strategy that provides a step-wise analysis of the similarity in overall gene expression profiles between individual samples. The relationship is presented graphically in a dendogram (Fig. 2), where samples cluster closer to each other the more their respective gene expression profiles resemble one another. As shown in Figure 2, all POAG samples clustered together on one side of the dendogram, whereas three of four normal samples clustered on the other side of the dendogram, suggesting that differences in the expression profile correlated with the existence of POAG in the sample and were not random. TM sample N138, a normal control that clustered with glaucoma samples, was derived from a patient who had eye surgery for the implantation of an intraocular lens shortly before death. In this type of surgery, there is a routine use of glucocorticoid-containing eye drops. Glucocorticoids have been known for many years to cause a specific steroid-induced form of POAG[19] and thus may be the reason that this donor's TM expressed genes in a manner similar to that of POAG samples. Also, cataract surgery may have caused a stress response resulting in IL1 secretion,[20] leading to a gene expression pattern similar to POAG TM. TM sample G123, which was derived from a patient with low-tension glaucoma, clustered with the POAGs. TM samples from patients G125 and G131 who had suspected glaucoma clustered together with the normal group. TM sample G125 was derived from a patient with pseudoexfoliative syndrome which may predispose the eye to POAG but does not constitute a full-blown POAG by itself.[21] Indeed, the patient was given the diagnosis of glaucoma only a short time before death and at the time of death showed no cupping of the optic nerve head with an IOP <21 mm Hg without medication (Table 1). TM sample G131 was derived from a patient with suspected narrow-angle glaucoma, a condition that is an anatomic deformity that obstructs aqueous outflow but does not generally correlate with TM cell dysfunction.[22]

Identification of Differentially Expressed Genes in TM Derived from POAG Eyes

The present study had a two-tiered goal: to find out whether patients with POAG have a distinct pattern of gene expression that distinguishes them from normal subjects and the non-POAG glaucomas and to look into any pattern that emerges from the analysis to elucidate possible mechanisms of the pathogenesis of the disease. To achieve these goals, we first used TM from eyes with glaucoma of various etiologies and normal control subjects and performed an unsupervised hierarchical clustering by sample. These analyses revealed that POAG TM has a distinct gene expression profile that sets it apart from normal and non-POAG TM (Fig. 2). Using a BRB-ArrayTools class comparison *t*-test, we then analyzed POAGs versus normal subjects only, since non-POAG glaucomas are various biological entities that could not be grouped for any meaningful conclusion. This analysis identified sixty differentially expressed genes (>1.1-fold change, $P < 0.05$) between the normal and POAG groups. The 60 differentially expressed genes were visualized by using Cluster and Tree View software for heat map creation (Fig. 3). As shown in Figure 3, in a graphical representation of gene expression profiles of these 60 genes, POAG and normal samples show a distinct profile of gene expression. Together, data presented in Figures 2 and 3 suggest that POAG samples form a distinct group, characterized by a specific gene expression pattern that is likely to be relevant to the disease process. For further analyses, genes were defined as differentially expressed if there was a

>1.4-fold difference between the normal and POAG groups. Using this threshold, we pared the list of 60 statistically significant genes down to 19 genes to be used in further analyses (Table 2). Although a detection call filter was not applied to the raw data, 18 genes at the 1.4-fold change level showed "present" detection in at least one probeset on the array for all three POAG samples, despite some cases of very low RMA signal intensities (<25). For clarity, genes listed in Table 2 are grouped according to their involvement in specific cellular processes, as determined by the DAVID software. Of these 19 differentially expressed genes, the expression of 13 was upregulated and that of 6 genes was downregulated in POAG TM compared with normal TM (Table 2); 10 are glycogenes, and the remaining are either cytokines and their receptors (CCL2, CCL5, IL6R) or growth factors and their receptors (PDGFRB, BMP4, MST1); and 26% fell in the cell-adhesion category, 21% in apoptosis, 47% in cell communication and 31% in macromolecule metabolism with some genes falling in more than one category.

RT-qPCR Confirmation of Differentially Expressed Genes

We used gene-specific RT-qPCR to confirm the differential expression of five selected genes. We chose these genes only because they are differentially expressed and can be taken as examples to confirm the reliability of the microarray data. A housekeeping gene, β-actin, served as the control. For the most part, the RT-qPCR data were in agreement with those obtained by array hybridization. In general, for genes measured by RT-qPCR, the mRNA levels were shown to change in the same direction as the changes measured by the microarray detection (Fig. 4A). PECAM-1, lumican, activin A, and P-selectin, which were found to be upregulated in POAG specimens by microarray, were all detected in higher amounts in the POAG specimens compared with normal subjects, by RT-qPCR. Compared with microarray analysis, the change (*x*-fold) detected by RT-qPCR was higher for PECAM-1 lumican and P-selectin, similar for activin A, and lower for ICAM-1 (Fig. 4A). As described earlier, E-selectin has been shown to be a marker for glaucomatous TM. Analysis of hybridization intensities for the individual probes of the human E-selectin probe set revealed very high background noise, suggesting that the E-selectin probe set in the GLYCOv2 array was defective. Therefore, it was not possible to asses the E-selectin expression pattern in the present study by microarray hybridization. However, we did compare E-selectin expression levels in normal and POAG samples by RT-qPCR. As seen in Figure 4B, like P-selectin which was shown to be differentially expressed in our microarray data, E-selectin showed profoundly elevated expression levels in POAG samples compared with normal samples.

Discussion

In the present study, gene array technology was used for the first time to examine differential gene expression in the TM of POAG eyes. For this study, a custom microarray (Affymetrix), GLYCOv2, focused on genes participating in carbohydrate-based recognition systems, was used. This analysis focused on transcriptional regulation of carbohydrate-binding proteins, glycosyltransferases, glycosidases, carbohydrate sulfotransferases, and sulfatases as well as selected cytokines and growth factors. The GLYCOv2 array is a robust tool because it has three probe sets for every glycogene, each of which comprises 11 oligonucleotides and 11 mismatched counterparts for control, bringing the overall level of scrutiny to 33 times per gene. Combining this with the use of at least three different TM specimens for each group, we attribute a high level of confidence to our findings that were further validated by RT-PCR.

As described earlier, to date, global gene expression studies in TM have compared normal TM tissue or cultured cells to models of POAG involving cells treated with dexamethasone or TGFβ, or whole TM tissue harvested from eyes in organ culture after perfusion at high pressure. Clearly, the present study involving evaluation of gene expression in the whole tissue, as

opposed to cultured cells, and of diseased sample versus normal sample as opposed to model sample versus normal sample brings us a step closer to observing the in vivo disease condition.

Comparison of gene expression profiles of normal and POAG TM revealed that POAG TM tissues have a unique glycogene expression pattern that defines them as a group distinct from normal. Indeed, some of the genes that we found to be differentially expressed were found in model systems as well. For example, mimecan and activinA, which were found to be elevated in POAG in the present study, have been reported to be upregulated by treatment of TM with TGFβ.[4] In contrast, clusterin which has been shown to be elevated in response to dexamethasone treatment[2] was found to be down-regulated in all POAG specimens analyzed in the present study. This is not surprising, considering that there is no indication that the POAG samples used in the present study were derived from patients incurring glaucoma as a result of corticosteroid exposure. In addition, corticosteroid exposure may not induce the same results in situ and in culture. For instance, dexamethasone treatment of cultured rat thymocytes causes elevation in clusterin expression[23] but in vivo dexamethasone does not affect clusterin expression in the rat thymus.[24] Another gene, MCP-1 which has been shown to be downregulated in TM cells treated with TGFβ,[4] was found to be upregulated in all three POAG specimens analyzed in this study. This too is not surprising, because TGFβ has been shown to inhibit NFκB signaling in nonocular systems.[25] Because MCP-1 is a target of NFκB, it is reasonable to expect that TGFβ treatment of normal cells would result in decreased expression of MCP-1. Based on the same reasoning, if NFκB is constitutively activated in POAG TM, as has been shown before,[15] an increased expression of NFκB targets such as MCP-1 would be expected. Significantly, our study has identified a novel set of genes that are reported herein for the first time to be differentially expressed between normal and POAG TM. Although it is beyond the scope of this report to highlight the potential significance of each altered gene, some genes are of unique interest and warrant specific mention. It has previously been reported that the glycosaminoglycan (GAG) content of TM extracellular matrix is altered in POAG. The keratan sulfate (KS) GAG content is reduced in POAG TM, and the chondroitin sulfate (CS) GAG content is elevated.[26] Our results suggest a putative feedback mechanism responding to this aberrant GAG composition. We found that the expression of lumican, the core protein of KS proteoglycan and of α 1,6 fucosyltransferase (FUT8), an enzyme responsible for core fucosylation of *N*-glycans of keratan sulfate as well as other oligosaccharide chains, is upregulated in POAG TM. Lumican has been shown to induce apoptosis of keratocytes, and it has been shown that corneal keratocytes derived from lumican-null mice show a significant increase in proliferation and a decreased rate of apoptosis in situ and in culture compared with keratocytes derived from wild-type mice. These effects are reversed when cultured cells are made to express recombinant human lumican and keratocyte proliferation is reduced in the presence of exogenous recombinant human lumican in culture media.[27] Thus, it is logical to hypothesize that increased lumican expression in TM cells of POAG eyes may, at least in part, be responsible for reduced TM cell density that is known to be associated with POAG.[28]

As stated earlier, it has been reported that CS content of GAG is elevated in POAG.[26] The present study revealed that iduronate-2-sulfatase (IDS), an enzyme participating in the degradation of CS, shows increased levels of expression in POAG TM, while chondroitin 4-O-sulfotransferase, involved in the biosynthesis of CS, showed reduced levels of expression in POAG TM. Chondroitin 4-O-sulfotransferase is responsible for the specific 4-O sulfation of chondroitin. The method used in published studies[26] for assessment of the GAG composition in normal and POAG TM used digestion by ABC chondroitin sulfate lyase. This approach cannot differentiate between 4-O sulfated, 6-O sulfated, and nonsulfated CS proteoglycans. It is therefore possible that, although there is an overall elevation in the levels of CS proteoglycans in POAG TM, these have a different sulfation pattern, such as a shift from 4-O sulfation to 6-O sulfation or an overall reduction in sulfation. Such a shift from 4-O sulfated CS to predominantly 6-O sulfated or nonsulfated CS GAGs has been found in scoliotic

cartilage[29] and in pancreatic and various other types of carcinomas.[30] Although the exact effect of these sulfation pattern changes is still not well understood, it is possible that it plays a role in changing the ECM in a manner conducive to disease.

Another gene with an elevated level of expression in POAG TM is the TGFβ family member activinA (inhibin βA). This gene was also found to be upregulated in TM by TGFβ_1 and by TGFβ_2 treatments.[4] Activins have been shown to be expressed in a tissue- and process-specific manner, such that they are differentially expressed in various tissues during development,[31] wound healing,[32] and pregnancy.[33] They play diverse roles in key biological processes including cell cycle arrest and apoptosis[34] and have been shown to stimulate nuclear localization of NFκB.[35] The diverse roles of activins in these key biological processes and the possible involvement of these functions in the pathogenesis of POAG make them an interesting subject for further study.

A unique inflammation-independent stress response has been reported to function in glaucomatous TM. In this positive feedback loop, glaucomatous TM cells constitutively secrete IL-1α and show nuclear localization of NFκB.[15] In this respect, it is noteworthy that several of the genes that we found to have elevated expression in POAG have been shown to be NFκB targets in nonocular studies. These include MCP-1,[36] RANTES,[37] PECAM1,[38] and P-selectin.[39] PECAM1 and P-selectin are membrane-spanning lectins that serve both as cell adhesion molecules and as signaling receptors. PECAM1 has recently been implicated in a negative-feedback loop in which its cross-linking leads to downregulation of NFκB activity in activated endothelial cells.[40] It would be interesting to know whether activation of PECAM1 exerts a similar function in TM cells. In nonocular cells, activation of P-selectin by antibody cross-linking has been shown to transduce signals into endothelial cells, causing Ca^{2+} spikes, stress fiber formation, and morphologic changes.[41] Because drugs that affect the cytoskeleton cause a reduction in outflow resistance,[42] it is reasonable to expect that activation of P-selectin by countereceptors may have an effect on outflow facility.

We found that the expression of the receptor for IL6 is elevated in POAG TM. In this regard, it has been shown that IL6 expression is elevated in TM in response to elevated IOP[5] and in a certain type of neovascular glaucoma.[43] IL6, a cytokine that mediates inflammatory responses, is known to increase the permeability of blood vessels. Thus, it is tempting to speculate that activation of IL6 signaling may have an impact on outflow facility.[5] The present study revealed that the expression of the PDGFβ receptor is reduced in POAG. PDGFβ has been shown to stimulate proliferation in TM cells,[44] to induce expression of various matrix metalloproteinases,[45] and to enhance TM phagocytic activity,[46] all of which are crucial functions of TM cells and are vital for the maintenance of proper outflow facility. The decrease in PDGFβ receptor expression in POAG TM cells may perturb many of the PDGFβ-mediated functions, ultimately resulting in a reduction in outflow facility. In the present study, the expression of BMP2 and -4 (considered the same gene by some databases, but submitted under different accession numbers) was found to be downregulated in POAG. BMP2 and -4 and their receptors have previously been reported in the human TM.[47] A mouse with a heterozygous deficiency for the BMP4 gene shows anterior segment dysgenesis and elevated IOP. These abnormalities are very similar to those in developmental glaucoma[48] suggesting that a reduction in the BMP4 gene product is deleterious to the TM and to outflow facility.

It is important to determine whether one or more differentially expressed genes identified in the present study have the potential to serve as diagnostic markers of glaucoma. At present, the diagnosis of POAG is made by routine tonometry and by inspection of the optic nerve heads.[49] However, these methods are limited in diagnosis of the very early phase of POAG. During the early phase, IOP may not be significantly elevated, the optic nerve head may have little or no abnormalities, and POAG may still exist in the eye. By contrast, a molecular marker

that differentiates glaucomatous TM from normal TM may help diagnose the disease at an early stage, before identifiable optic nerve head damage has occurred. Better yet, a multigene expression signature that can distinguish diseased tissue from normal would probably be more accurate and reduce the occurrence of false-positive diagnoses. Such signatures are in the process of development for the prognosis of treatment outcomes in various types of cancer.[50–53] As useful and accurate as such a diagnostic tool may be, it is hard to imagine routine biopsies performed on TM for diagnostic purposes. Data generated from studies such as the current one may ultimately lead to the development of noninvasive approaches to diagnose the disease in the early phase. P-selectin, a cell adhesion lectin, identified in this study as overexpressed by POAG TM, has a soluble form, as does E-selectin which has been identified as a marker for glaucomatous TM and was validated by the present study. The soluble forms of P- and E-selectins have been found in serum in levels reflective of a disease state in various diseases[54–59] including eye diseases.[60,61] It is feasible then that the serum levels of these adhesion molecules may reflect the state of the TM in patients and may serve as diagnostic markers.

In summary, the data presented in this communication strongly suggest involvement of carbohydrate-based recognition systems in the pathogenesis of glaucoma and identifies genes with differential expression between the normal and POAG tissue that makes them worthy of further investigation designed to understand the pathogenic mechanisms and identify diagnostic markers for glaucoma.

Acknowledgements

The authors thank Teresa Borras for helpful comments and James Flynn for help with RT-qPCR.

References

1. Leung YF, Tam PO, Lee WS, et al. The dual role of dexamethasone on anti-inflammation and outflow resistance demonstrated in cultured human trabecular meshwork cells. Mol Vis 2003;9:425–439. [PubMed: 12963864]
2. Lo WR, Rowlette LL, Caballero M, et al. Tissue differential microarray analysis of dexamethasone induction reveals potential mechanisms of steroid glaucoma. Invest Ophthalmol Vis Sci 2003;44:473–485. [PubMed: 12556371]
3. Ishibashi T, Takagi Y, Mori K, et al. cDNA microarray analysis of gene expression changes induced by dexamethasone in cultured human trabecular meshwork cells. Invest Ophthalmol Vis Sci 2002;43:3691–3697. [PubMed: 12454038]
4. Zhao X, Ramsey KE, Stephan DA, Russell P. Gene and protein expression changes in human trabecular meshwork cells treated with transforming growth factor-beta. Invest Ophthalmol Vis Sci 2004;45:4023–4034. [PubMed: 15505052]
5. Gonzalez P, Epstein DL, Borras T. Genes upregulated in the human trabecular meshwork in response to elevated intraocular pressure. Invest Ophthalmol Vis Sci 2000;41:352–361. [PubMed: 10670462]
6. Vittitow J, Borras T. Genes expressed in the human trabecular meshwork during pressure-induced homeostatic response. J Cell Physiol 2004;201:126–137. [PubMed: 15281095]
7. Hernandez JD, Baum LG. Ah, sweet mystery of death!—galectins and control of cell fate. Glycobiology 2002;12:127R–136R.
8. Yang RY, Liu FT. Galectins in cell growth and apoptosis. Cell Mol Life Sci 2003;60:267–276. [PubMed: 12678492]
9. Horiguchi N, Arimoto K, Mizutani A, et al. Galectin-1 induces cell adhesion to the extracellular matrix and apoptosis of non-adherent human colon cancer COLO201 cells. J Biochem (Tokyo) 2003;134:869–874. [PubMed: 14769876]
10. Perillo NL, Marcus ME, Baum LG. Galectins: versatile modulators of cell adhesion, cell proliferation, and cell death. J Mol Med 1998;76:402–412. [PubMed: 9625297]

11. Kuwabara I, Sano H, Liu FT. Functions of galectins in cell adhesion and chemotaxis. Methods Enzymol 2003;363:532–552. [PubMed: 14579602]
12. Cao Z, Zhao Z, Mohan R, et al. Role of the lewis(x) glycan determinant in corneal epithelial cell adhesion and differentiation. J Biol Chem 2001;276:21714–21723. [PubMed: 11278542]
13. Kojima N, Fenderson BA, Stroud MR, et al. Further studies on cell adhesion based on le(x)-le(x) interaction, with new approaches: embryoglycan aggregation of f9 teratocarcinoma cells, and adhesion of various tumour cells based on le(x) expression. Glycoconj J 1994;11:238–248. [PubMed: 7841799]
14. Hughes RC. Galectins as modulators of cell adhesion. Biochimie (Paris) 2001;83:667–676.
15. Wang N, Chintala SK, Fini ME, Schuman JS. Activation of a tissue-specific stress response in the aqueous outflow pathway of the eye defines the glaucoma disease phenotype. Nat Med 2001;7:304–309. [PubMed: 11231628]
16. Sawaguchi S, Yue BY, Chang IL, et al. Ascorbic acid modulates collagen type i gene expression by cells from an eye tissue—trabecular meshwork. Cell Mol Biol 1992;38:587–604. [PubMed: 1303307]
17. Wilson CL, Pepper SD, Hey Y, Miller CJ. Amplification protocols introduce systematic but reproducible errors into gene expression studies. Biotechniques 2004;36:498–506. [PubMed: 15038166]
18. Skrypina NA, Timofeeva AV, Khaspekov GL, et al. Total RNA suitable for molecular biology analysis. J Biotechnol 2003;105:1–9. [PubMed: 14511905]
19. Kersey JP, Broadway DC. Corticosteroid-induced glaucoma: a review of the literature. Eye. ePub ahead of print, May 6, 2005
20. Wang N, Chintala SK, Fini ME, Schuman JS. Ultrasound activates the tm elam-1/il-1/nf-kappab response: a potential mechanism for intraocular pressure reduction after phacoemulsification. Invest Ophthalmol Vis Sci 2003;44:1977–1981. [PubMed: 12714632]
21. Ritch, R. Exfoliation syndrome. In: Ritch, R.; Shields, MB.; Krupin, T., editors. The Glaucomas. 2. 2. St. Louis: Mosby; 1996. p. 993-1015.
22. Ritch, R.; Lowe, RF. Angle-closure glaucoma: mechanisms and epidemiology. In: Ritch, R.; Shields, MB.; Krupin, T., editors. The Glaucomas. 2. 2. St. Louis: Mosby; 1996. p. 801-819.
23. Bettuzzi S, Troiano L, Davalli P, et al. In vivo accumulation of sulfated glycoprotein 2 mRNA in rat thymocytes upon dexamethasone-induced cell death. Biochem Biophys Res Commun 1991;175:810–815. [PubMed: 2025255]
24. French LE, Sappino AP, Tschopp J, Schifferli JA. Clusterin gene expression in the rat thymus is not modulated by dexamethasone treatment. Immunology 1994;82:328–331. [PubMed: 7927505]
25. Wang W, Huang XR, Li AG, et al. Signaling mechanism of TGF-beta1 in prevention of renal inflammation: role of SMAD7. J Am Soc Nephrol 2005;16:1371–1383. [PubMed: 15788474]
26. Knepper PA, Goossens W, Hvizd M, Palmberg PF. Glycosaminoglycans of the human trabecular meshwork in primary open-angle glaucoma. Invest Ophthalmol Vis Sci 1996;37:1360–1367. [PubMed: 8641839]
27. Vij N, Roberts L, Joyce S, Chakravarti S. Lumican suppresses cell proliferation and aids FAS-FAS ligand mediated apoptosis: implications in the cornea. Exp Eye Res 2004;78:957–971. [PubMed: 15051477]
28. Alvarado J, Murphy C, Juster R. Trabecular meshwork cellularity in primary open-angle glaucoma and nonglaucomatous normals. Ophthalmology 1984;91:564–579. [PubMed: 6462622]
29. Theocharis AD, Karamanos NK, Papageorgakopoulou N, et al. Isolation and characterization of matrix proteoglycans from human nasal cartilage: compositional and structural comparison between normal and scoliotic tissues. Biochim Biophys Acta 2002;1569:117–126. [PubMed: 11853965]
30. Theocharis AD, Tsara ME, Papageorgacopoulou N, et al. Pancreatic carcinoma is characterized by elevated content of hyaluronan and chondroitin sulfate with altered disaccharide composition. Biochim Biophys Acta 2000;1502:201–206. [PubMed: 11040445]
31. Thompson TB, Cook RW, Chapman SC, et al. Beta a versus beta b: is it merely a matter of expression? Mol Cell Endocrinol 2004;225:9–17. [PubMed: 15451562]
32. Sulyok S, Wankell M, Alzheimer C, Werner S. Activin: an important regulator of wound repair, fibrosis, and neuroprotection. Mol Cell Endocrinol 2004;225:127–132. [PubMed: 15451577]

33. Florio P, Luisi S, Ciarmela P, et al. Inhibins and activins in pregnancy. Mol Cell Endocrinol 2004;225:93–100. [PubMed: 15451573]
34. Woodruff TK. Regulation of cellular and system function by activin. Biochem Pharmacol 1998;55:953–963. [PubMed: 9605419]
35. Sugatani T, Alvarez UM, Hruska KA. Activin a stimulates ikappab-alpha/nfkappab and rank expression for osteoclast differentiation, but not akt survival pathway in osteoclast precursors. J Cell Biochem 2003;90:59–67. [PubMed: 12938156]
36. Rovin BH, Dickerson JA, Tan LC, Hebert CA. Activation of nuclear factor-kappa b correlates with MCP-1 expression by human mesangial cells. Kidney Int 1995;48:1263–1271. [PubMed: 8569088]
37. Mori N, Krensky AM, Geleziunas R, et al. Helicobacter pylori induces RANTES through activation of NF-kappa b. Infect Immun 2003;71:3748–3756. [PubMed: 12819056]
38. Botella LM, Puig-Kroger A, Almendro N, et al. Identification of a functional NF-kappa b site in the platelet endothelial cell adhesion molecule-1 promoter. J Immunol 2000;164:1372–1378. [PubMed: 10640752]
39. Pan J, McEver RP. Regulation of the human P-selectin promoter by BCL-3 and specific homodimeric members of the NF-kappa b/REL family. J Biol Chem 1995;270:23077–23083. [PubMed: 7559449]
40. Cepinskas G, Savickiene J, Ionescu CV, Kvietys PR. PMN transendothelial migration decreases nuclear NFkappab in IL-1beta-activated endothelial cells: role of PECAM-1. J Cell Biol 2003;161:641–651. [PubMed: 12743110]
41. Kaplanski G, Farnarier C, Benoliel AM, et al. A novel role for E- and P-selectins: Shape control of endothelial cell monolayers. J Cell Sci 1994;107:2449–2457. [PubMed: 7531200]
42. Clark AF, Miggans S, Wilson K, et al. Cytoskeletal changes in cultured human glaucoma trabecular meshwork cells. J Glaucoma 1995;4:183–188.
43. Chen KH, Wu CC, Roy S, et al. Increased interleukin-6 in aqueous humor of neovascular glaucoma. Invest Ophthalmol Vis Sci 1999;40:2627–2632. [PubMed: 10509659]
44. Wordinger RJ, Clark AF, Agarwal R, et al. Cultured human trabecular meshwork cells express functional growth factor receptors. Invest Ophthalmol Vis Sci 1998;39:1575–1589. [PubMed: 9699547]
45. Alexander JP, Samples JR, Acott TS. Growth factor and cytokine modulation of trabecular meshwork matrix metalloproteinase and TIMP expression. Curr Eye Res 1998;17:276–285. [PubMed: 9543636]
46. Tamura M, Iwamoto Y. The effect of platelet-derived growth factor on phagocytosis of cultured human trabecular cells. Exp Eye Res 1989;48:761–770. [PubMed: 2731573]
47. Wordinger RJ, Agarwal R, Talati M, et al. Expression of bone morphogenetic proteins (BMP), BMP receptors, and BMP associated proteins in human trabecular meshwork and optic nerve head cells and tissues. Mol Vis 2002;8:241–250. [PubMed: 12131877]
48. Chang B, Smith RS, Peters M, et al. Haploinsufficient BMP4 ocular phenotypes include anterior segment dysgenesis with elevated intraocular pressure. BMC Genet 2001;2:18. [PubMed: 11722794]
49. Epstein, DL. Primary open angle glaucoma. In: Allingham, RR.; Schuman, JS., editors. Glaucoma. 4. 1. Baltimore, MD: Williams and Wilkins; 1997. p. 183-198.
50. Rabson AB, Weissmann D. From microarray to bedside: Targeting NF-{kappa}b for therapy of lymphomas. Clin Cancer Res 2005;11:2–6. [PubMed: 15671521]
51. Robison JE, Perreard L, Bernard PS. State of the science: molecular classifications of breast cancer for clinical diagnostics. Clinical Biochemistry 2004;37:572–578. [PubMed: 15234238]
52. Pusztai L, Hess KR. Clinical trial design for microarray predictive marker discovery and assessment. Ann Oncol 2004;15:1731–1737. [PubMed: 15550577]
53. Hinshaw MA, Wood GS. cDNA microarrays: revolutionary technology for the diagnosis, prognosis, and treatment of cutaneous t-cell lymphoma. Int J Dermatol 2005;44:181–183. [PubMed: 15807722]
54. Gearing AJ, Hemingway I, Pigott R, et al. Soluble forms of vascular adhesion molecules, E-selectin, ICAM-1, and VCAM-1: pathological significance. Ann NY Acad Sci 1992;667:324–331. [PubMed: 1285023]
55. Coata G, Pennacchi L, Bini V, et al. Soluble adhesion molecules: marker of pre-eclampsia and intrauterine growth restriction. J Matern Fetal Neonatal Med 2002;12:28–34. [PubMed: 12422906]

56. Kvasnicka T, Kvasnicka J, Ceska R, et al. Increasing plasma levels of soluble cell adhesion molecules (SE-selectin, SP-selectin and SICAM-1) in overweight adults with combined hyperlipidemia. Sb Lek 2001;102:473–477. [PubMed: 12448198]

57. Furui J, Ishii M, Ikeda H, et al. Soluble forms of the selectin family in children with Kawasaki disease: prediction for coronary artery lesions. Acta Paediatr 2002;91:1183–1188. [PubMed: 12463316]

58. Furui J. Soluble forms of P-, E- and L-selectin in children with Kawasaki disease. Kurume Med J 2001;48:135–143. [PubMed: 11501494]

59. O'Hanlon DM, Fitzsimons H, Lynch J, et al. Soluble adhesion molecules (E-selectin, ICAM-1 and VCAM-1) in breast carcinoma. Eur J Cancer 2002;38:2252–2257. [PubMed: 12441261]

60. Kulig G, Pilarska K. The role of adhesion molecules in the pathogenesis of graves ophthalmopathy. Klin Oczna 2001;103:147–150. [PubMed: 11873415]in Polish

61. Matsumoto K, Sera Y, Ueki Y, et al. Comparison of serum concentrations of soluble adhesion molecules in diabetic microangiopathy and macroangiopathy. Diabet Med 2002;19:822–826. [PubMed: 12358868]

A

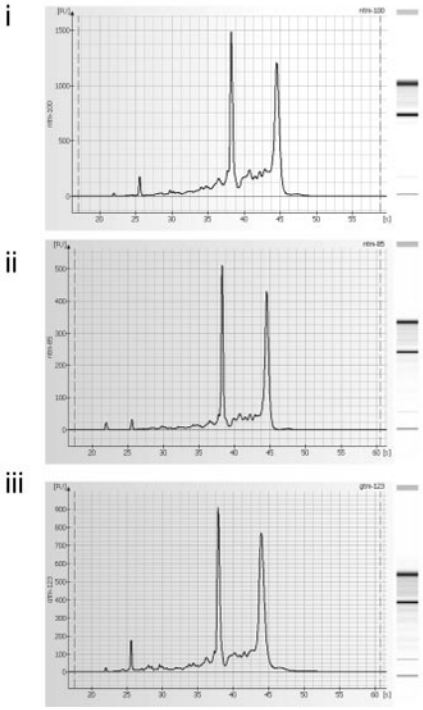

B

Specimen code	Total RNA yield (ng)	28S/18S ratio
P85	90	1.2
P99	143	1.2
P133	203	1.2
G123	985	1.2
G125	1072	1.1
G131	1915	1
N100	338	1.1
N105	444	1.1
N134	105	1
N138	235	1.2

Figure 1.

The RNA quality from normal and glaucoma TM tissues was satisfactory. (**A**) Representative electropherograms and gel-like images of RNA preparations of normal (**Ai**), POAG (**Aii**), and non-POAG glaucoma (**Aiii**) samples. In all samples, the 18S and 28S gel bands and graph peaks were dominant. (**B**) 28S-18S ratios and yield of all RNA preparations.

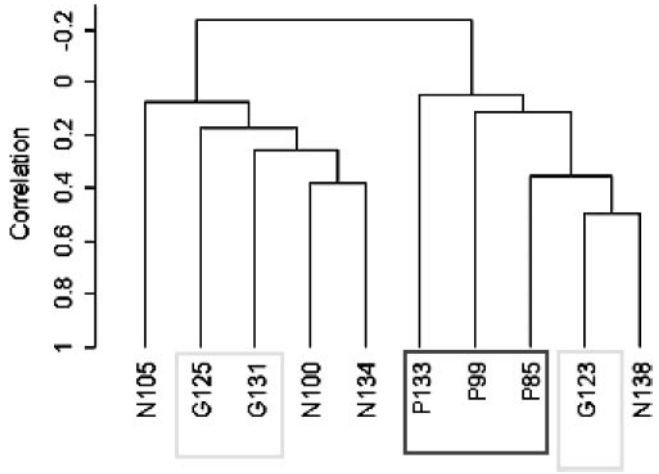

Figure 2.

Dendogram showing hierarchical cluster analysis of TM gene expression profiles of donors with POAG (P133, P99, P85), low-tension glaucoma (G123), or suspected glaucoma (G125, G131) and normal control subjects (N105, N100, N134, N138). The individual samples were clustered in branches of the dendogram based on overall similarity in patterns of gene expression. All POAG samples clustered together.

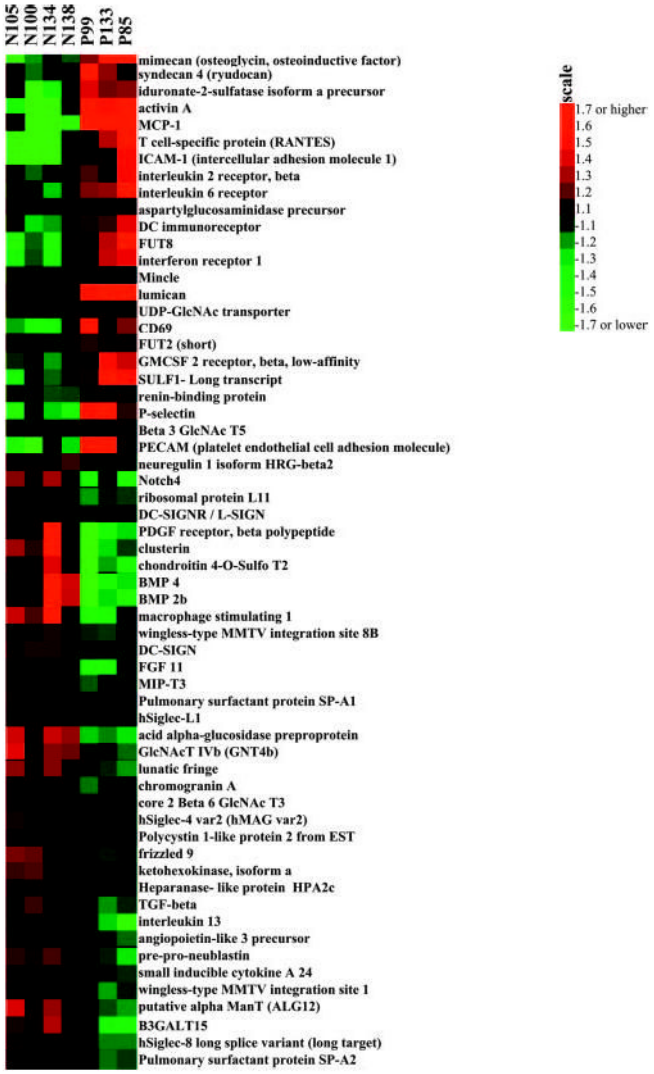

Figure 3.

Heat map of 60 differentially expressed genes (change >1.1-fold; $P < 0.05$). All signals are compared with a median value, and change from the median is visually represented by a color assignment (scale at *right*). POAG samples and normal samples showed visibly distinct profiles of gene expression.

A

Gene name	Fold Change by microarray	Fold Change by RT-qPCR
P-selectin	1.9	12.7
LUM	2.3	5.83
PECAM1	2.0	4.42
INHBA	2.5	2.26
ICAM1	2.1	1.17

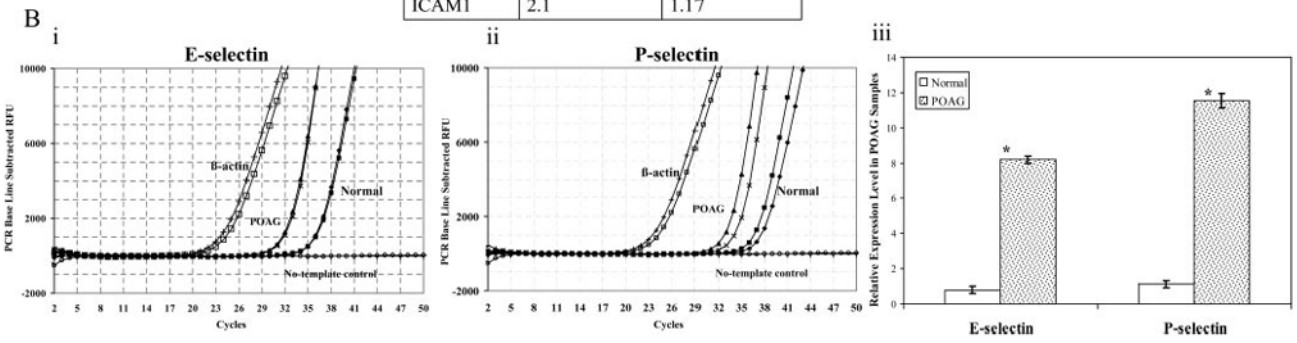

Figure 4.

RT-qPCR results supported the microarray data and showed overexpression of E-selectin in POAG samples. (**A**) Table comparing *x*-fold change of five genes as evaluated by microarray and RT-qPCR ($n = 6$ or more derived from at least two different specimens). (**Bi**, **Bii**) Original amplification plots of E- and P- selectin mRNAs showing significantly higher signals in POAG specimens compared with normal specimens. (**Biii**) The data were normalized against β-actin and the *x*-fold change was calculated, with NTM 105 used as a calibrator ($n = 6$ or more derived from at least two different specimens). *$P < 0.05$ compared with normal.

Table 1

Specimen Code, Age, and Clinical Findings for Donor Eyes

Category	Ocular Diagnosis	Specimen Code	Age (y)	Sex	Ocular Medication	Nonocular Diagnosis	Last-Measured Intraocular Pressure	Cup/Disc Ratio
POAG	POAG	P85	73	F	Betaxalol and artificial Tears	Lymphadenopathy, possible lymphoma	OD 14, OS 08	OD 0.6; OS 0.9
	POAG	P99	71	F	Timolol maleate	Coronary artery disease	Not available	Not available
	POAG	P133	86	F	Latanoprost, brimonidine	Hypertension, hypothyroid, renal mass	OD 44, OS 16	OD 1, OS 0.75
Low tension glaucoma	Low-tension glaucoma	G123	87	F	Bimatoprost at bed time and brimonidine P OU twice daily	Multiple myeloma	OD 10, OS 10	0.9 OU
Suspected glaucoma	Pseudoexfoliative glaucoma (suspected)	G125	81	M	Travoprost OS	Hypertension, myocardial infarction	OD 18, OS 15	1–2 OU
	Narrow-angle glaucoma(suspected)	G131	82	M	None	Lung fibrosis, coronary artery disease	OD 14, OS 13	OD 0.2, OS 0.2
Normal	None	N100	66	M	None	Esophageal cancer, pneumonia	NA	NA
	None	N105	70	M	None	Pneumonia, anemia, renal insufficiency, hypertension	NA	NA
	None	N134	84	F	None	Diverticulitis, colitis	NA	NA
	None	N138	86	F	None	CVA, gastrointestinal bleeding	NA	NA

CVA, cerebrovascular accident.

Table 2

Genes Differentially Expressed in POAG TM Compared with Normal TM

Category	Gene Name	Common Name	Geometric Mean of Intensities in Normal	Geometric Mean of Intensities In POAG	Change(*X*-fold)	Parametric *P*
Apoptosis	*CCL2*	Monocyte chemotactic protein(MCP-1)	58.1	226.7	3.9	0.0037
	INHBA	Inhibin, beta A (activin A)	46.1	115.5	2.5	0.0131
	SULF1	Extracellular sulfatase 1	12.4	21.4	1.7	0.0408
	CLU	Complement cytolysis inhibitor(clusterin)	2075	1186.9	−1.7	0.0489
Cell adhesion	*CCL5*	T-cell–specific protein (RANTES)	26.3	67.2	2.5	0.0331
	ICAM1	Intercellular adhesion molecule1(ICAM1)	46.6	98	2.1	0.0355
	PECAM1	Platelet endothelial cell adhesion molecule (PECAM1)	55	110.6	2.0	0.0427
	SELP	P-selectin (PADGEM)	20.8	40.2	1.9	0.0235
ECM GAG composition	*LUM*	Keratan sulfate proteoglycan(lumican)	7.8	17.9	2.3	0.0179
	FUT8	α (1,6) fucosyltransferase	29.6	44.9	1.5	0.0477
	IDS	Iduronate-2-sulfatase	65.9	99.5	1.5	0.0203
	CHST12	Chondroitin 4-O-sulfotransferase 2	189.4	124.2	−1.5	0.0217
Cell proliferation	*OGN*	Osteoglycin (mimecan)	315.6	592.5	1.9	0.0105
	PDGFRB	PDGF receptor	319.6	191.7	−1.7	0.0385
	BMP4[*]	Bone morphogenetic protein 2B(BMP 2b)	616.2	371	−1.7	0.0150
	(*BMP2B*)	Bone morphogenetic protein 4(BMP 4)	642.5	397.4	−1.6	0.0216
	MST1	Macrophage-stimulating factor 1(HGF-like)	188.6	125.9	−1.5	0.0351
	CD69	Early T-cell-activation antigen	8.9	13.1	1.5	0.0159
Cell communication	*IL6R*	Interleukin 6 receptor	12.7	18.7	1.5	0.0189

Genes are considered differentially expressed when there is a difference of 1.4-fold or more between the geometric mean signal of the POAG group (n = 3) and the normal group (n = 4).

[*] BMP4 and BMP2B are the same gene, submitted under different accession numbers.